Supporting Information

A DPA-based highly selective and sensitive fluorescent probe for mercuric ions and its imaging in living cells

Junhua Jia,[a] Luling Wu,[b] Yu Ding,[a] Chusen Huang,*[b] Weiping Zhu,*[a] Yufang Xu[a] and Xuhong Qian[a]

[a] State key Laboratory of Bioreactor Engineering, Shanghai Key Laboratory of Chemical Biology, School of Pharmacy, East China University of Science and Technology, Shanghai 200237, China. Fax: +86 21 6425 2603; Tel: +86 21 6425 3822; E-mail: wpzhu@ecsut.edu.cn
[b] The Education Ministry Key Laboratory of Resource Chemistry and Shanghai Key Laboratory of Rare Earth Functional Materials, Department of Chemistry, College of Life and Environmental Sciences, Shanghai Normal University, 100 Guilin Road, Shanghai 200234, China. E-mail: huangcs@shnu.edu.cn.

Table of Contents:

1. Materials and Instruments

All solvents were commercial without further purification. ^{1}H NMR spectra and ^{13}C NMR spectra were recorded in $CDCl_3$ and DMSO-d_6 with TMS as internal standard at 25 ^{o}C on a Bruker AV-400 spectrometer. pH titration was carried out by using a pH-Meter PB-10. All reactions were monitored by thin-layer chromatography (TLC) using UV-light (254 nm) and Flu-light (365nm). Mass spectra Electrospray ionization (ESI) mass spectrometry was carried out in a HP 1100 LC-MS spectrometer. Deionized water was purified using a Millipore Milli-Q A10 super-water system. HERA cell CO_2 and Multiskan Spectrum from Thermo Scientific. Leica TCS SP5 II Confocal Laser Scanning Microscope, 63x1.4 oil.Silica gel (300–400 mesh, Qingdao Haiyang Chemical Co., Ltd.) was used for column chromatography. All reagents were obtained commercially and used without further purification unless stated otherwise. Solvents such as dichloromethane (DCM), ethanol (EtOH), acetonitrile (CH_3CN) were the analytical grade. The salts used in stock aqueous solutions of metal ions ($LiClO_4$, $NaClO_4$, $Mg(ClO_4)_2$, $Ca(ClO_4)_2$, $Cd(ClO_4)_2 \cdot 6H_2O$, $Hg(ClO_4)_2 \cdot 3H_2O$,$Cr(ClO_4)_3 \cdot 6H_2O$, $KClO_4$, $AgClO_4$, $Zn(ClO_4)_2 \cdot 6H_2O$, $Co(ClO4)_2 \cdot 6H_2O$, $Cu(ClO_4)_2 \cdot 6H_2O$, $Ni(ClO_4)_2 \cdot 6H_2O$ and $Pb(ClO_4)_2 \cdot 3H_2O$) were purchased from Energy Chemical. Dulbecco's modified eagle medium (DMEM) and fetal calf serum were purchased from Hyclone. Pancreatin was purchased from SuoLaiBao, and MTT and DMSO were purchased from Sigma.

2. Synthesis

The structure of the fluorescent probes was shown in Scheme S1, and their synthetic route was depicted in Scheme S2.

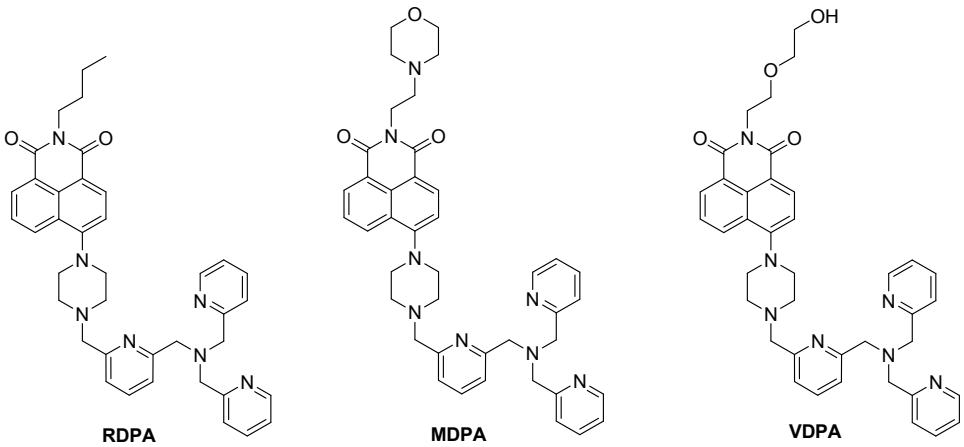

Scheme S1 Structures of **RDPA**, **MDPA** and **VDPA**

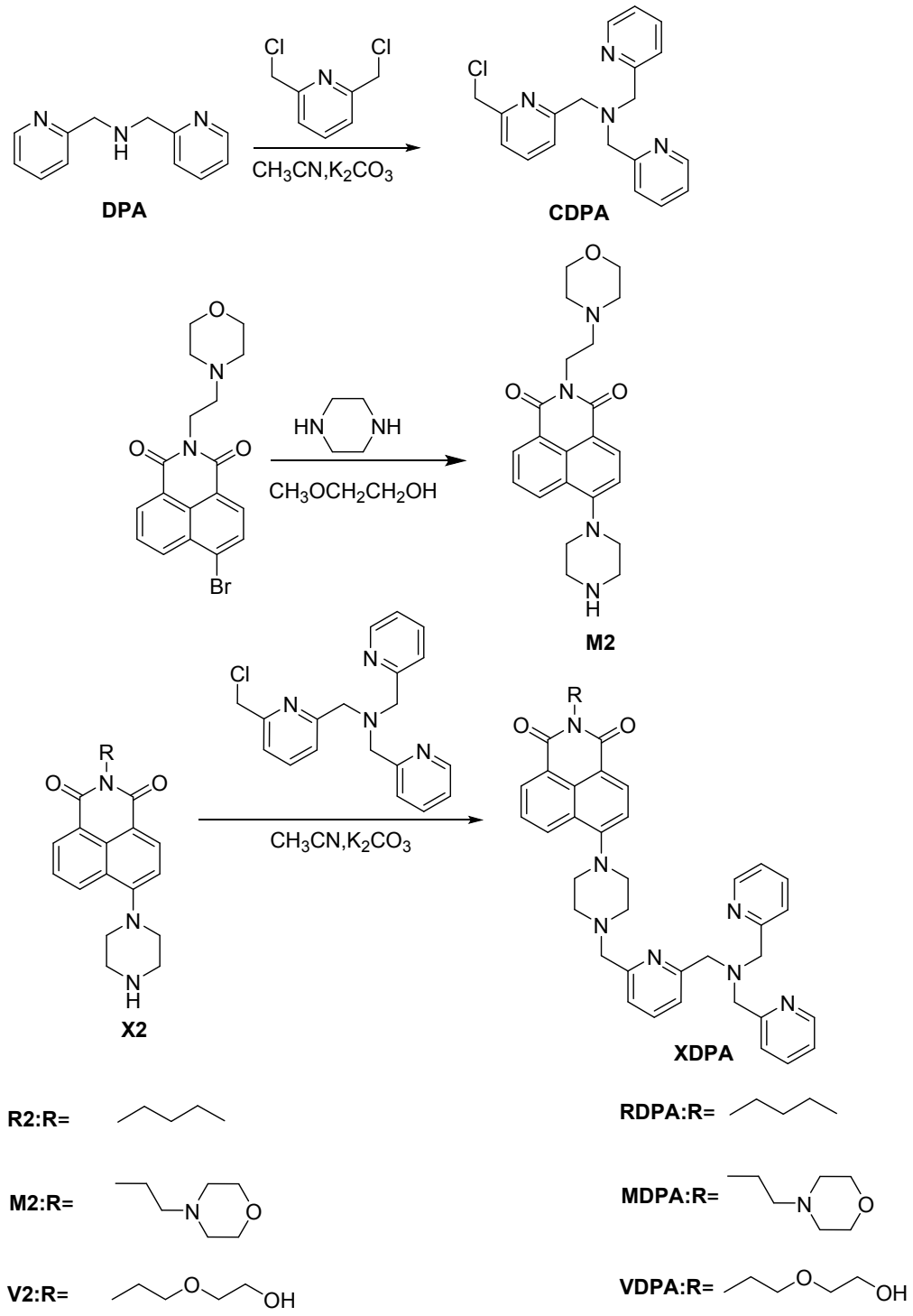

Scheme S2. Synthetic routes of fluorescent probes **RDPA**, **MDPA** and **VDPA**

General synthetic method to prepare RDPA, MDPA and VDPA

Synthesis of M2

N-(morpholinoethylamino)-4-bromo-1,8-naphthalimide (2 g, 5.15 mmol) and piperazine (664 mg, 7.7 mmol) were dissolved in 20 mL of 2-methoxyethanol, and the solution was refluxed for 10 h in argon atmosphere. After cooling to room temperature, the reaction mixture was evaporated by vacuum-rotary and the crude product was purified by column chromatography (DCM/MeOH=20/1) to give **M2** as a yellow solid, yield: 80%.

^{1}H NMR (400 MHz, $CDCl_3$) δ 8.57 (d, *J* = 7.2 Hz, 1H), 8.51 (d, *J* = 8.0 Hz, 1H), 8.38 (d, *J* = 8.0 Hz, 1H), 7.72 (t, *J*=8.0 Hz, 1H), 7.32–7.22 (m, 1H), 4.32 (t, *J* = 7.0 Hz, 2H), 3.69 (t, *J* = 4.0 Hz, 4H), 3.40 (s, 8H), 2.70 (t, *J* = 7.0 Hz, 2H), 2.60 (s, 4H).^{13}C NMR (100 MHz, $CDCl_3$) δ 164.35, 163.87, 155.55, 132.45, 131.19, 129.96, 129.83, 126.17, 125.96, 123.24, 117.19, 115.31, 77.41, 77.09, 76.78, 67.02, 56.16, 53.79, 52.96, 45.51, 37.09. MS (ES^+) calc. for $C_{22}H_{27}N_4O_3$ ($[M+H]^+$): 395.2083, found: 395.2072.

Synthesis of CDPA[1]

To the solution of compound 2,6-bis(chloromethyl)pyridine (4 g, 23 mmol) and potassium carbonate (900 mg, 6.5 mmol）in 80 mL acetonitrile, 2, 2-dipicolylamine **(DPA)** [2](1 mL, 5.9 mmol) was added with continuous stirring. The reaction mixture was then refluxed for 10 h. Reaction process was tracked by thin layer chromatography. Then the reaction mixture was evaporated by vacuum-rotary and purified through column chromatography over silica gel (DCM/MeOH=20/1) to give gray solid, yield: 60%.

^{1}H NMR (400 MHz, $CDCl_3$) δ 8.53 (d, *J* = 4.7 Hz, 2H), 7.74–7.62 (m, 3H), 7.58 (d, *J* = 7.8 Hz, 2H), 7.54 (d, *J* = 7.8Hz, 1H), 7.33 (d, *J* = 7.6 Hz, 1H), 7.18–7.09 (m, 2H), 4.65 (s, 2H), 3.90 (s, 6H). ^{13}C NMR (100 MHz, $CDCl_3$) δ 159.27, 159.19, 155.86, 149.10, 137.45, 136.47, 123.04, 122.22, 122.06, 121.04, 60.20, 59.96, 46.80. MS (ES^+) calc. for $C_{19}H_{20}N_4Cl$ ($[M+H]^+$): 339.1376, found: 339.1379.

Synthesis of VDPA, RDPA, MDPA [3]

VDPA can be readily prepared by a simple reaction of **V2** and **CDPA** (Scheme S1). **CDPA** (101.7mg, 0.3 mmol）, **V2 (**170mg, 0.45 mmol）, anhydrous potassium carbonate (60 mg, 0.43 mmol）were dissolved in 20 mL acetonitrile，the mixture was stirred and refluxed for 10 h under argon atmosphere. Then the reaction mixture was evaporated by vacuum-rotary and purified through column chromatography over silica gel (DCM/MeOH=15/1) to give brown solid, yield:70%.

^{1}H NMR (400 MHz, $CDCl_3$) δ 8.54 (d, *J* = 7.2 Hz, 3H), 8.48 (d, *J* = 8.0 Hz, 1H), 8.38 (d, *J* = 8.0 Hz, 1H), 7.78-7.58 (m, 6H), 7.54 (d, *J* = 8.0 Hz, 1H), 7.36 (d, *J* = 8.0 Hz, 1H), 7.16 (dd, *J* = 12.0, 8.0 Hz, 3H), 4.42 (t, *J* = 6.0 Hz, 2H), 3.92 (d, *J* = 8.0 Hz, 6H), 3.83 (t, *J* = 8.0 Hz, 4H), 3.68 (dd, J_1= 12.0, J_2= 4.0 Hz, 4H), 3.30 (s, 4H), 2.84 (s, 4H).^{13}C NMR (100 MHz, DMSO-d_6) δ 163.52, 162.97, 158.97, 158.29, 157.40, 155.61, 148.81, 145.53, 137.01, 136.53, 132.18, 130.62, 129.07, 125.92, 125.18, 122.51, 122.40, 122.12, 121.16, 120.76, 115.33, 114.94, 72.06, 66.92, 63.63, 60.14, 59.39, 52.70, 52.61, 48.57.MS (ES^+) calc. for $C_{39}H_{42}N_7O_4$($[M+H]^+$): 672.3298 , found: 672.3299。

RDPA was synthesized via similar synthetic route of VDPA brown solid, yield 83%.

^{1}H NMR (400 MHz, $CDCl_3$) δ 8.61 – 8.46 (m, 4H), 8.39 (d, *J* = 8.4 Hz, 1H), 7.70-7.65 (m, 4H), 7.60 (d, *J* = 8.0 Hz, 2H), 7.52 (d, *J* = 8.0 Hz, 1H), 7.36 (d, *J* = 8.0 Hz, 1H), 7.19 (d, *J* = 8.0 Hz, 1H), 7.15 (dd, *J* = 12.0, 6.0 Hz, 2H), 4.16(t, *J* = 8.0 Hz, 2H), 3.92 (s, 2H), 3.91 (s, 2H),3.82 (s, 2H), 3.30 (s, 4H), 2.85 (s, 4H), 1.71-1.67 (m, 2H), 1.49-1.39 (m, 2H), 0.97 (t, *J* = 8.0 Hz, 3H). ^{13}C NMR (100 MHz, $CDCl_3$) δ 159.26, 158.80, 154.08, 153.69, 150.69, 143.84, 131.73, 131.23, 127.26, 125.79, 125.04, 124.59, 120.87, 120.36, 118.01, 117.72, 116.80, 116.22, 111.46, 109.62, 59.12 ,54.98, 48.06, 47.73, 34.82, 25.01, 15.15, 8.62. MS (ES+) calc. for $C_{39}H_{42}N_7O_2$ ($[M+H]^+$): 640.3393, found: 640.3400。

MDPA was also synthesized via similar synthetic route of VDPA brown solid, yield 80%.

^{1}H NMR (400 MHz, $CDCl_3$) δ 8.54 (t, *J* = 6.8 Hz, 3H), 8.49 (d, *J* = 8.0 Hz, 1H), 8.40 (d, *J* = 8.4

Hz, 1H), 7.67 (t, *J* = 7.2 Hz, 4H), 7.60 (d, *J* = 7.7 Hz, 2H), 7.52 (d, *J* = 7.6 Hz, 1H), 7.36 (d, *J* = 7.6 Hz, 1H), 7.20 (d, *J* = 8.1 Hz, 1H), 7.16 (t, *J* = 6.0 Hz,2H), 4.33 (t, *J* = 6.9 Hz, 2H), 3.92 (d, *J* = 8.5 Hz, 6H), 3.82 (s, 2H), 3.69 (s, 4H), 3.31 (s, 4H), 2.85 (s, 4H), 2.69 (t, *J* = 6.9 Hz, 2H), 2.60 (s, 4H).^{13}C NMR (100 MHz, $CDCl_3$) δ 164.47, 163.98, 159.28, 158.90, 157.43, 156.06, 149.06, 136.98, 136.48, 132.57, 131.08, 130.43, 129.87, 126.09, 125.60, 123.09, 122.98, 122.05, 121.54, 121.42, 116.45, 114.87, 67.00, 64.36, 60.27, 60.19, 56.17, 53.77, 53.29, 52.99, 37.02.MS (ES^+) calc. for $C_{41}H_{45}N_8O_3$ ($[M+H]^+$): 697.3615 , found: 697.3606

2. Methods

3.1 ^{1}H NMR Titration Experiments

To study the binding interaction of the probes with Hg^{2+} in solution, ^{1}H NMR spectra of **RDPA** were recorded in DMSO-d_6 upon gradual addition of varying concentrations of Hg^{2+} (in D_2O).

3.2 Spectroscopic Tests and Methods

A stock solution of **VDPA**, **RDPA**, and **MDPA** were prepared in CH_3CH_2OH at a concentration of 10^{-3} M, respectively. All of the metal ions for detections were prepared by pure water. The emission spectra of the probes in the presence of various metal ions were measured by excitation with 400 nm in a 1 cm path length quartz cuvette. The slit sizes for excitation and emission were both 5 nm.

According to Job's curve, **VDPA** and Hg^{2+} form the 1: 1 complex. The association constant Y of the complex was calculated according to the Benesi–Hildebrand equation.

$$Y = Y_0 + \frac{Y_{LIM} - Y_0}{2}\left\{1 + \frac{C_M}{C_L} + \frac{1}{K_S C_L} - \left[\left(1 + \frac{C_M}{C_L} + \frac{1}{K_S C_L}\right)^2 - 4\frac{C_M}{C_L}\right]^{\frac{1}{2}}\right\}$$

Y_{LIM}, Y_0, and Y are fluorescence intensities of **VDPA** in the presence of Hg^{2+} at saturation, free **VDPA**, and any intermediate Hg^{2+} concentration.

3.3 Fluorescence quantum yield for of VDPA and for Hg^{2+}

The quantum yield was measured at room temperature referenced to quinine sulfate in sulfuric acid aqueous solution (Φ_{F0}= 0.53(λ_{ex}=366 nm)) and calculated according to the following equation

$$\Phi_F = \Phi_{F0}\,(A_0/A)\,(F/F_0)$$

where Φ_F is the radiative quantum yield of the sample; Φ_{F0} is the radiative quantum yield of the standard; A and A_0 are the absorbance of the sample and standard at the excitation wavelength, respectively; F and F_0 are the integrated areas of the emission for the sample and standard, respectively.

3.4 Calculation of the detection limit

The detection limit was calculated based on the fluorescence titration. The emission intensity of **VDPA** without Hg^{2+} was measured 10 times and the standard deviation of blank measurements was determined. A good linear relationship between the maximum intensity of fluorescence emission and the Hg^{2+} concentration could be obtained in the 0-10 nM concentration range (R = 0.9959). The detection limit was then calculated with the equation: detection limit = $3\sigma/k$, where σ

is the standard deviation of blank measurements, *k* is the slope between intensity versus sample concentration. The detection limit of Hg^{2+} was measured to be 5.49 nM.

3.5 Fluorescent imaging and cytotoxicity assay.

Fluorescent imaging [4] Hela Cells were grown in the exponential phase of growth on 35 mm glass-bottom culture dishes (Φ 20 mm) for 1-2 days to reach 70-90% confluency. These cells were used for fluorescence imaging experiments. The cells were washed with DMEM for three times, and then incubated with 10 μM of probe in 2 mL DMEM (containing, 5% DMF)under an atmosphere of 5% CO_2 and 95% air for 30 min at 37 °C. Cells were washed twice with 1 mL PBS at room temperature, and then followed by addition of 1 mL PBS and observed under confocal microscopy (Leica TCS SP5 II Confocal Laser Scanning Microscope, 63x1.4 oil), with excitation by 405 nm laser and 500-700 nm emission light was collected. For the Hg^{2+} treated samples, the cells were washed with DMEM for three times, and then incubated with 10 μM of probe in 2 mL DMEM (containing 5% DMF)) under an atmosphere of 5% CO_2 and 95% air for 10 min at 37 °C. Then followed by addition of 20 μM of Hg^{2+}, which was further incubated for another 20 min. After the cells were washed twice with 1 mL PBS at room temperature, 1 mL PBS was added and observed under confocal microscopy, with excitation by 405 nm laser and 500-700 nm emission light was collected.

Cytotoxicity assay [5]The cytotoxic effects of **VDPA** were assessed through the MTT assay. Simply, Hela cells were seeded in 96-well microplates at a density of 8×10^4 cells/mL in 100 μL. After 24 h of cell attachment, media were removed and washed with DMEM and then various concentrations of probe (0-90 μM) made in DMEM were added to the cells and incubated for 12 h and 48 h. Cells in a culture medium without **VDPA** were used as the control. Three replicate wells were used for each control and test concentration. MTT (100 μL, 1 mg/mL) in DMEM was subsequently added to each well. The plates were then incubated at 37 °C for 4 h in a 5% CO_2 humidified incubator. The plate was shaken for 10 min, after the medium was carefully removed, and 150 μL DMSO was added. The absorbance was measured at 570 nm by a microplate reader. Cell proliferation rate shows the cell viability.

3. Figures

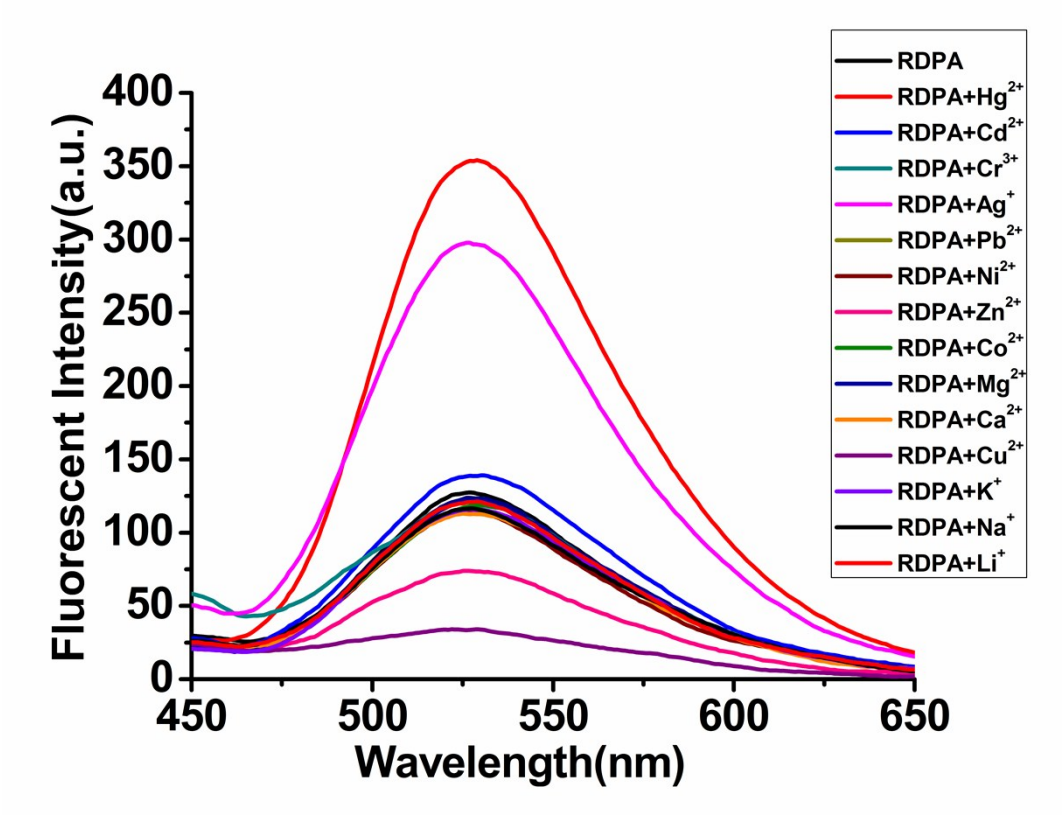

Fig S1. Fluorescence spectra of **RDPA** (10 μM, λ_{ex} = 400 nm) before and after the addition of various metal ions (100 μM) in ethanol /PBS buffer (v/v=1/1).

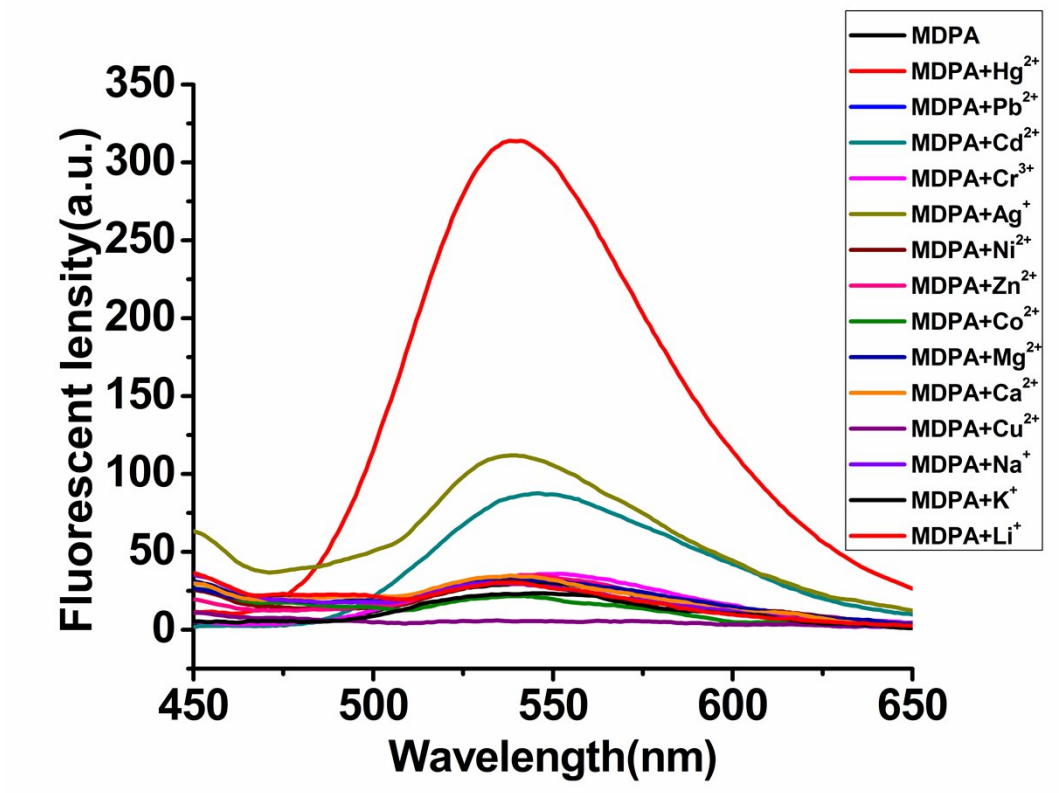

Fig S2. Fluorescence spectra of **MDPA** (10 μM, λ_{ex} = 400 nm) before and after the addition of various metal ions (100 μM) in ethanol /PBS buffer (v/v=1/9).

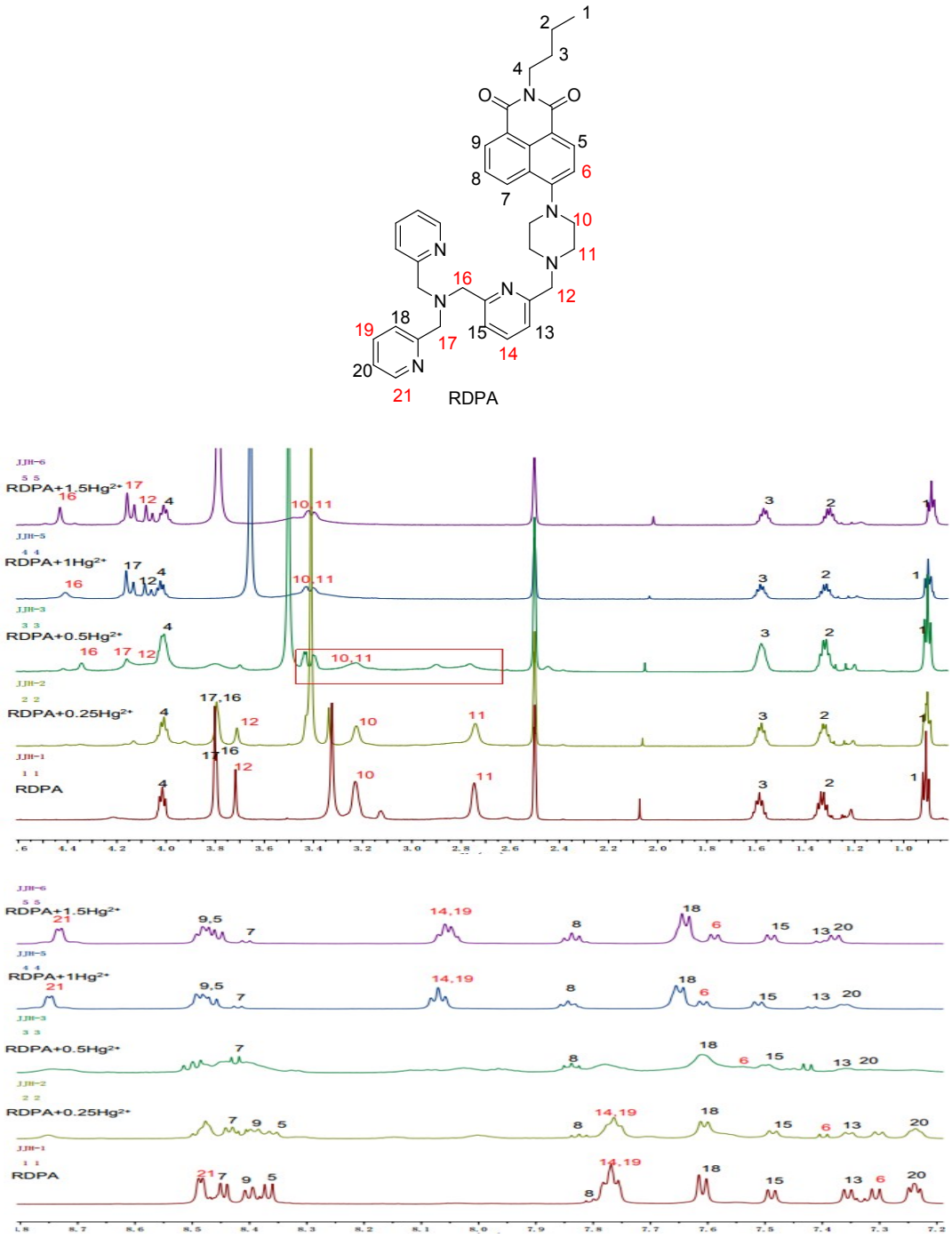

Fig S3. ^{1}H NMR titration experiments of **RDPA** with Hg^{2+} (in D_2O) in DMSO-d_6. Inset: The proton sequence number of **RDPA**.

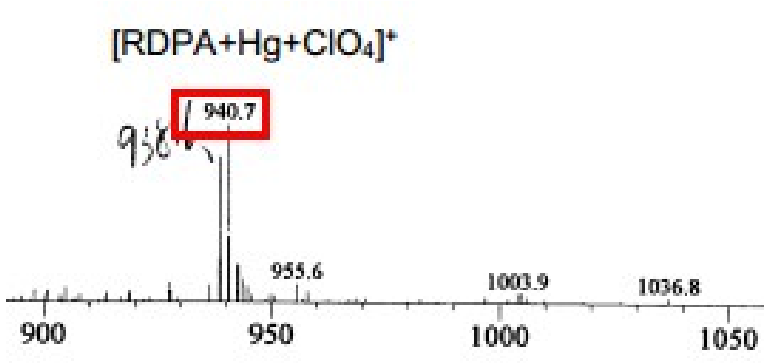

Fig S4. ESI-MS of **RDPA** in the presence of Hg^{2+} in CH_3CN and CH_3OH**.**

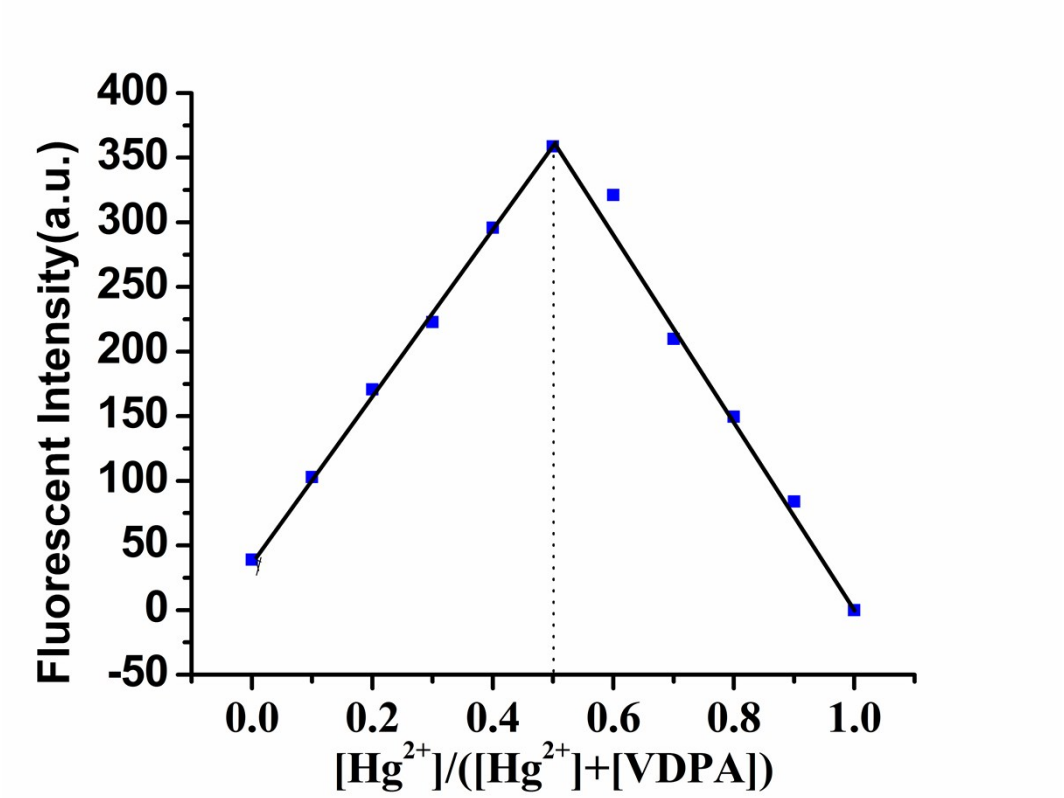

Fig S5. Job's plot for the binding of **VDPA** with Hg^{2+}, the total concentration of **VDPA** and Hg^{2+} is 20 μM.

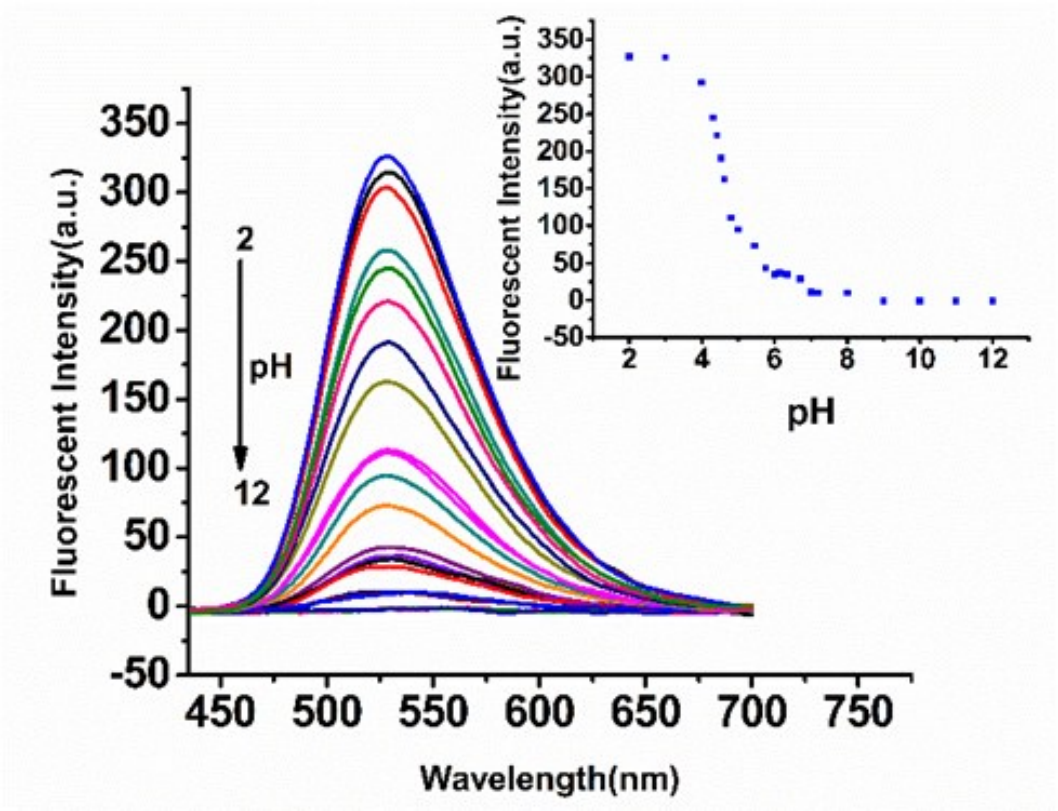

Fig S6. Fluorescence pH titration spectra of **VDPA** (adjusted by 1 M HCl or 1 M NaOH) in water solution. Inset: Fluorescence intensity changes of **VDPA** under different pH, λ_{ex} = 400 nm, λ_{em} =540 nm, 25 ^{o}C, water).

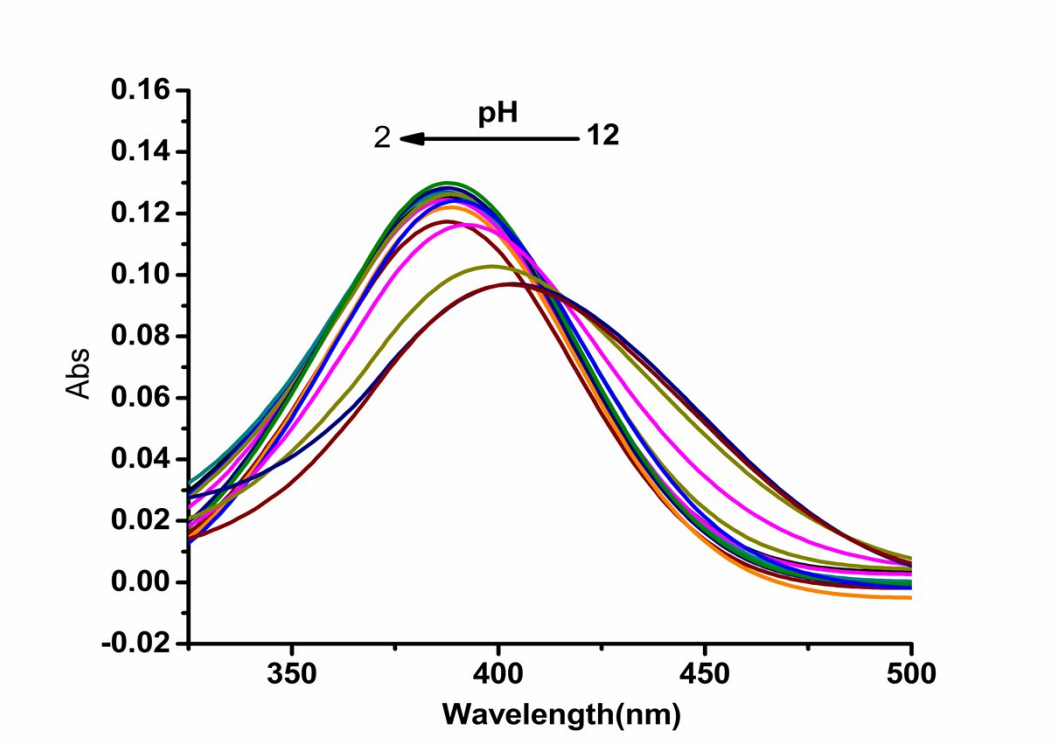

Fig S7. The absorption properties of **VDPA** on changing the pH

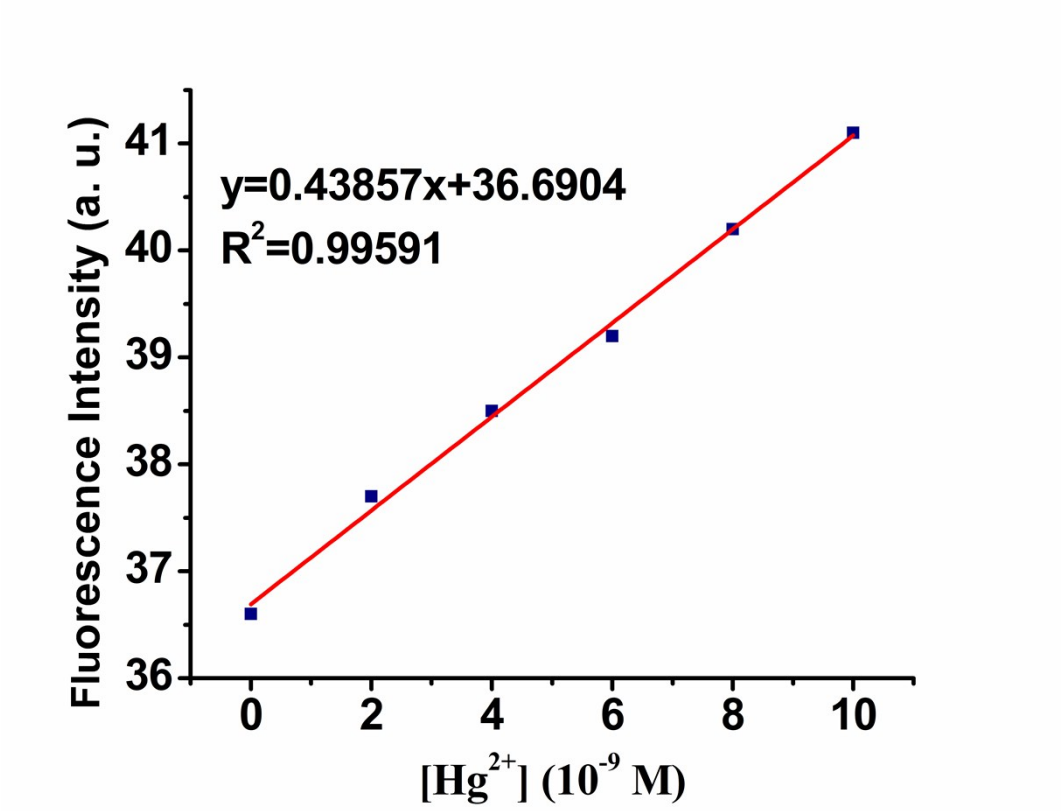

Fig S8. Normalized plot for determination of detection limit

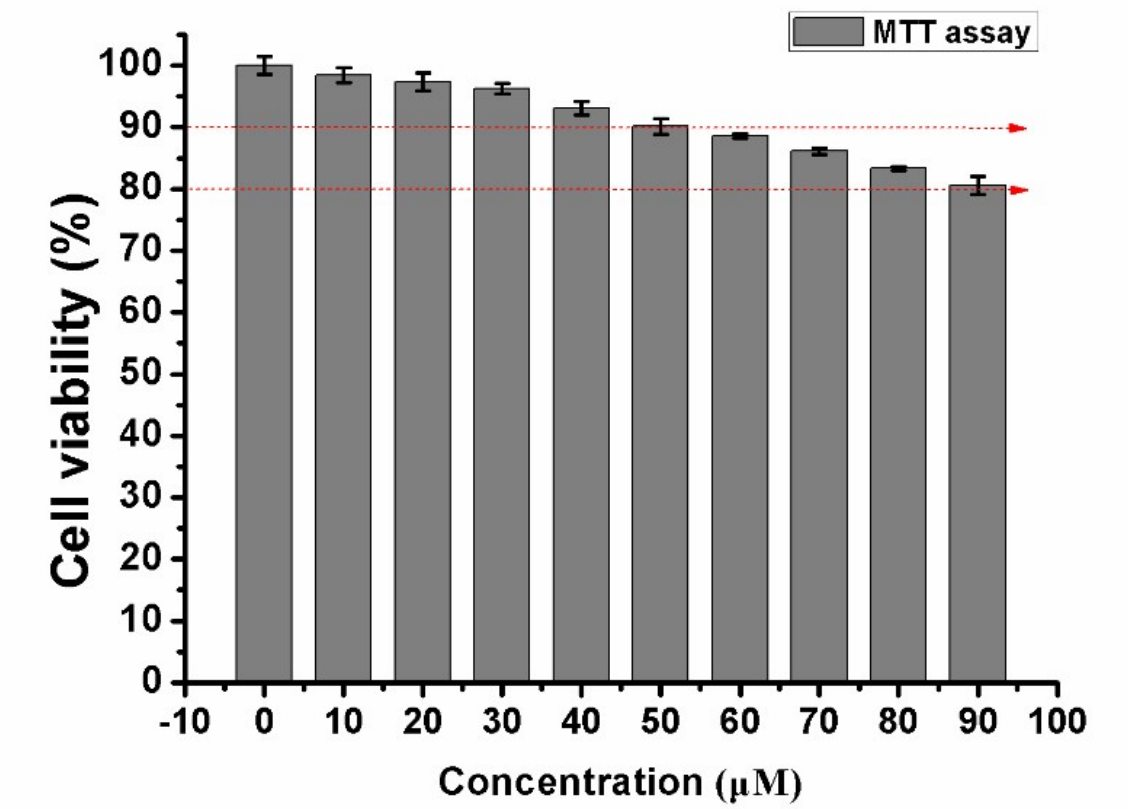

Fig S9. Cell viability of Hella cells treated with various concentrations (10 μM–90 μM) of **VDPA** for 12 h determined by MTT assay.

5. NMR and ESI spectra

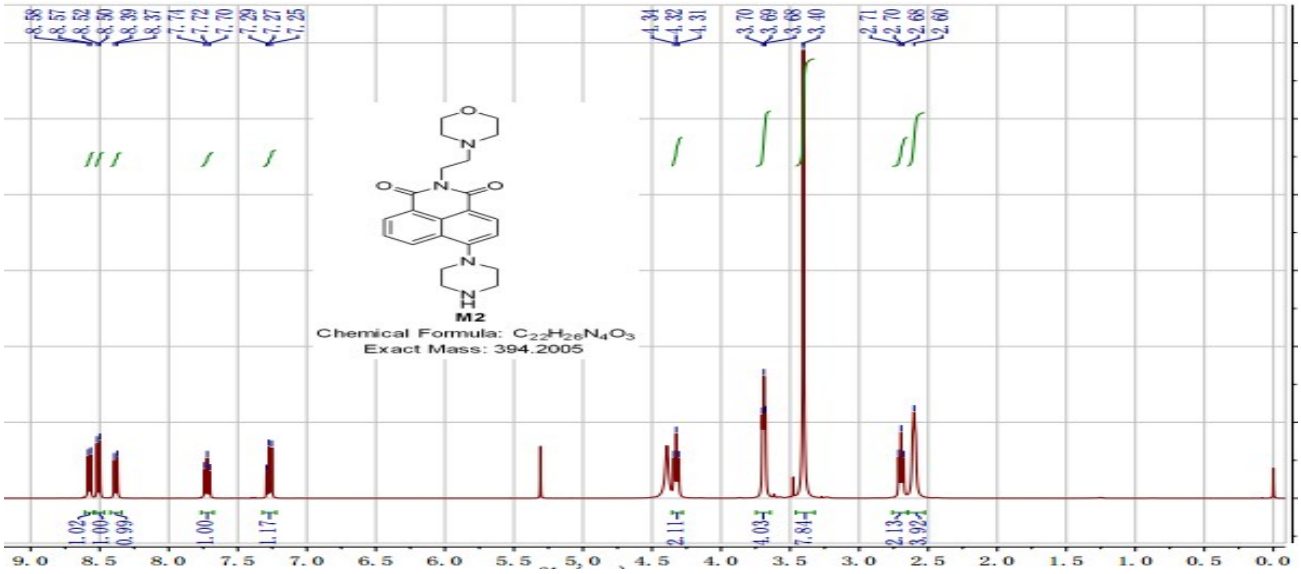

Fig S10. ^{1}H NMR spectrum of **M2** in $CDCl_3$.

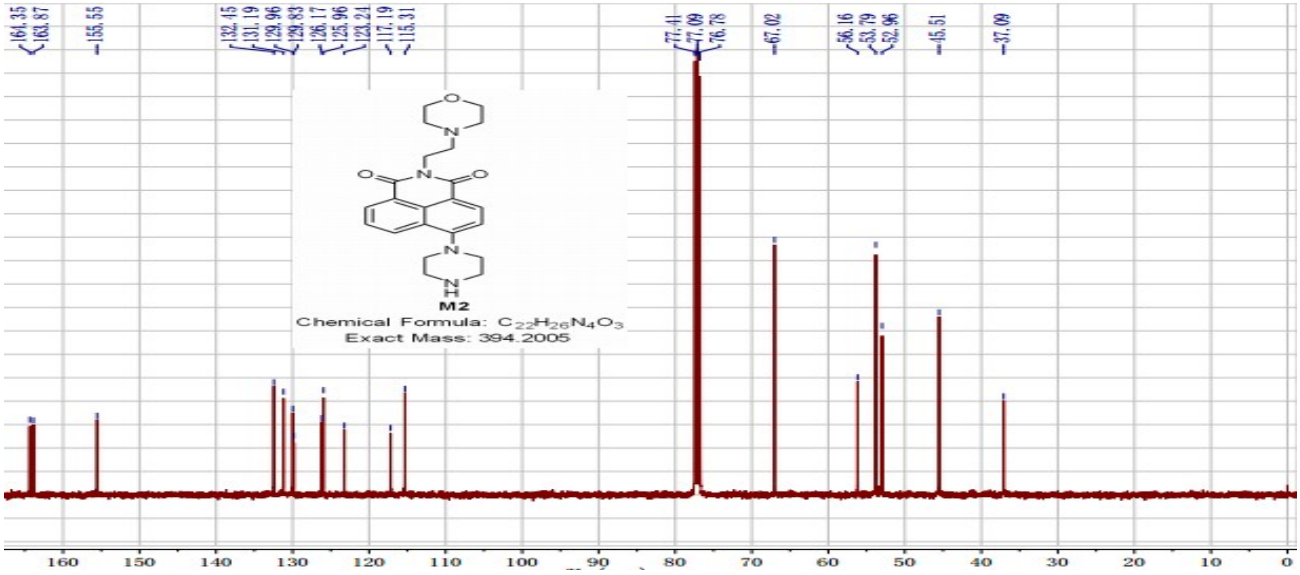

Fig S11. ^{13}C NMR spectrum of **M2** in $CDCl_3$.

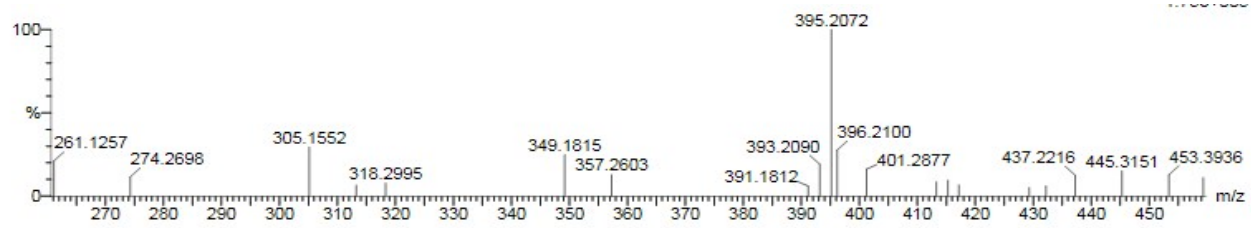

Minimum:				-1.5			
Maximum:		300.0	50.0	100.0			
Mass	Calc. Mass	mDa	PPM	DBE	i-FIT	i-FIT (Norm)	Formula
395.2072	395.2083	-1.1	-2.8	11.5	20.8	0.0	C22 H27 N4 O3

Fig S12. ESI-MS spectrum of **M2**

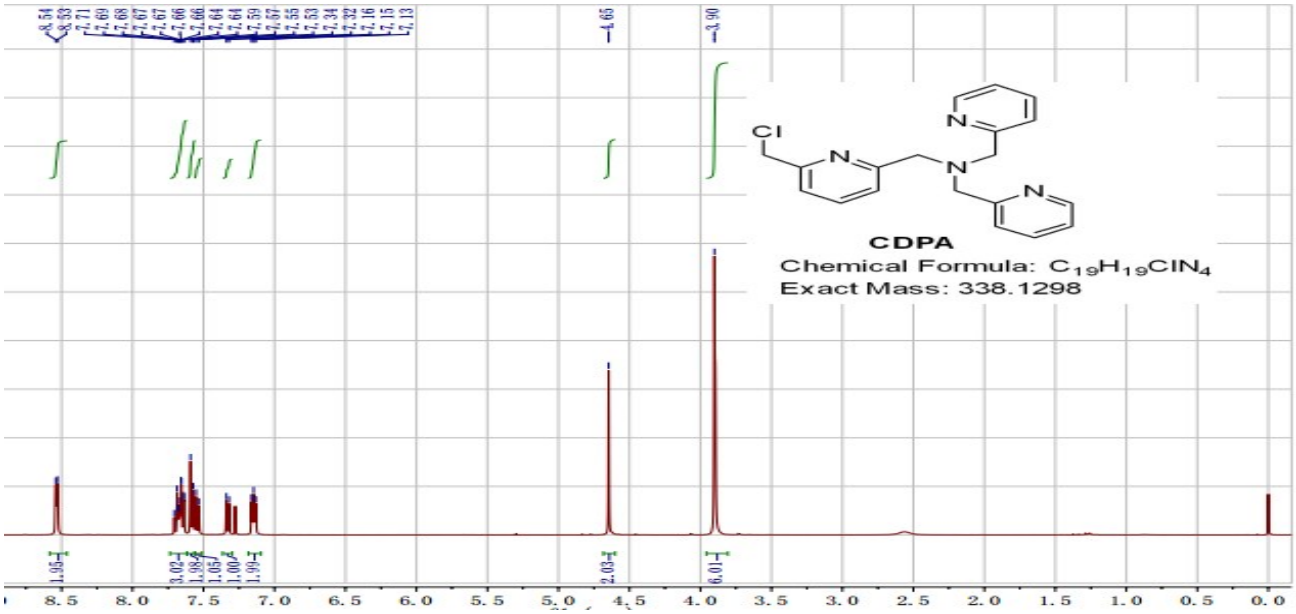

Fig S13. ^{1}H NMR spectrum of **CDPA** in $CDCl_3$.

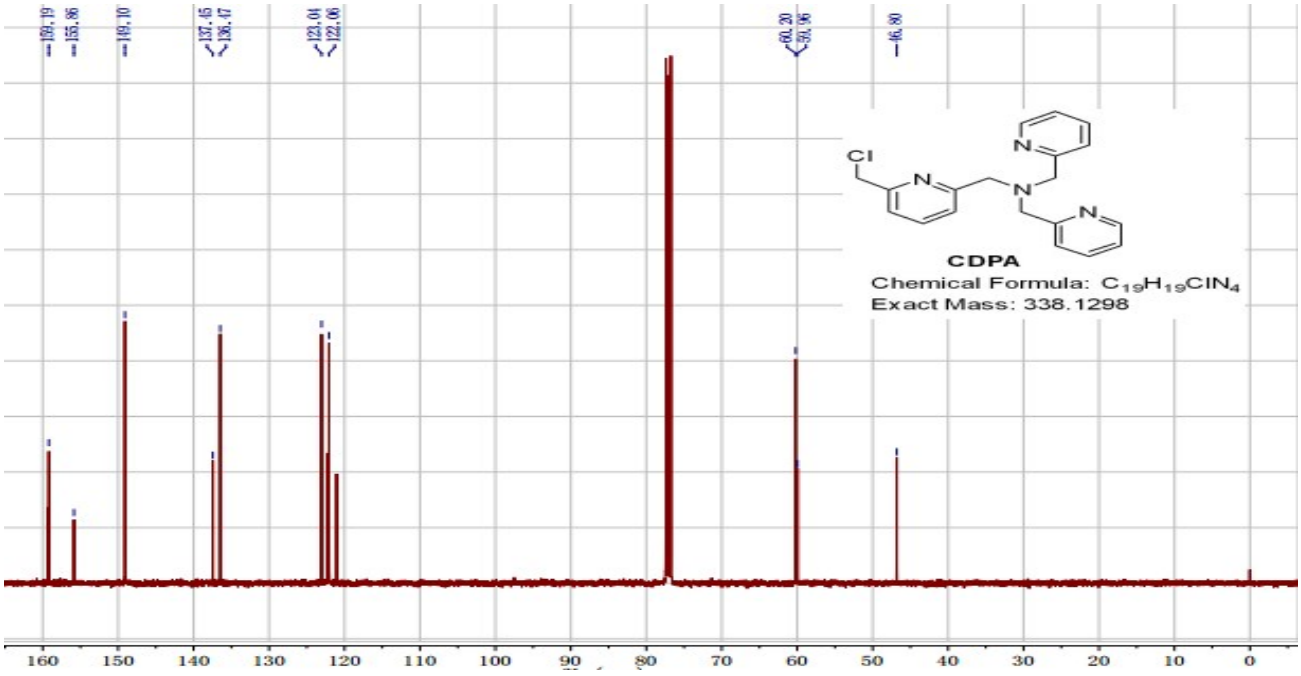

Fig S14. ^{13}C NMR spectrum of **CDPA** in $CDCl_3$.

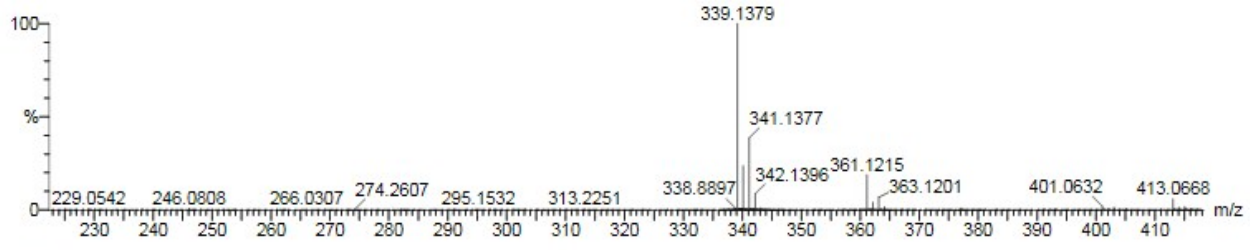

Minimum:				-1.5			
Maximum:		300.0	50.0	100.0			
Mass	Calc. Mass	mDa	PPM	DBE	i-FIT	i-FIT (Norm)	Formula
339.1379	339.1376	0.3	0.9	11.5	250.0	0.0	C19 H20 N4 Cl

Fig S15. ESI-MS spectrum of **CDPA**

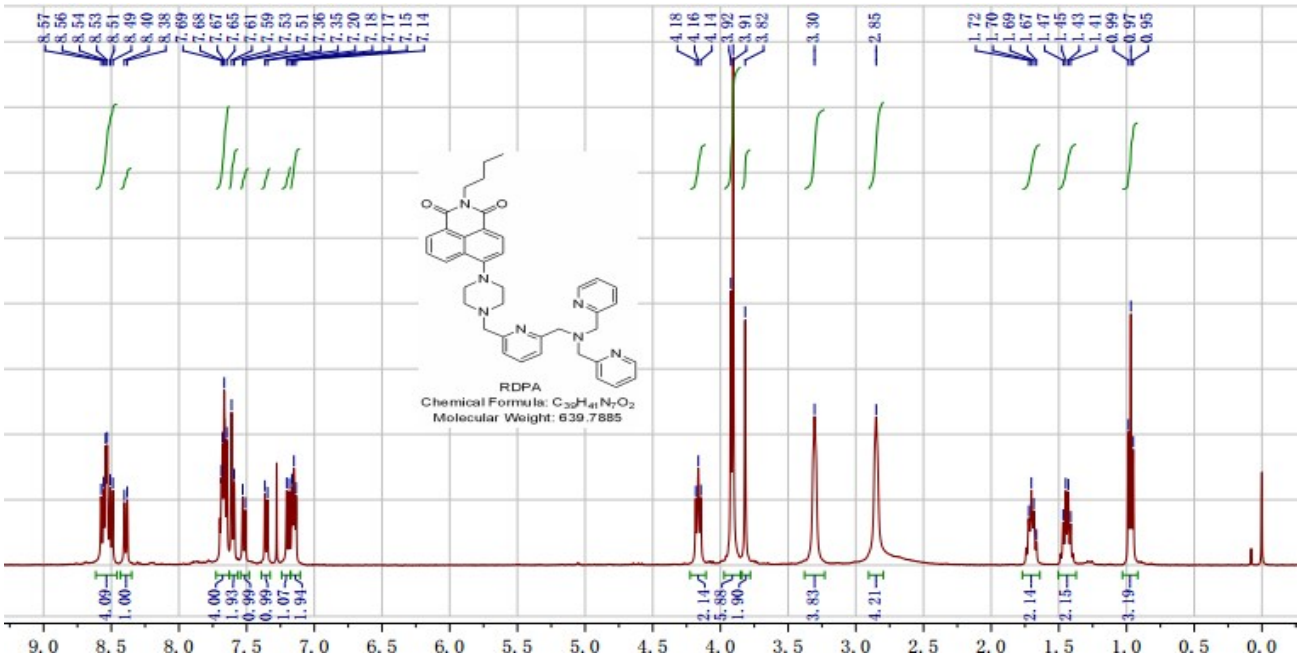

Fig S16. ^{1}H NMR spectrum of **RDPA** in $CDCl_3$.

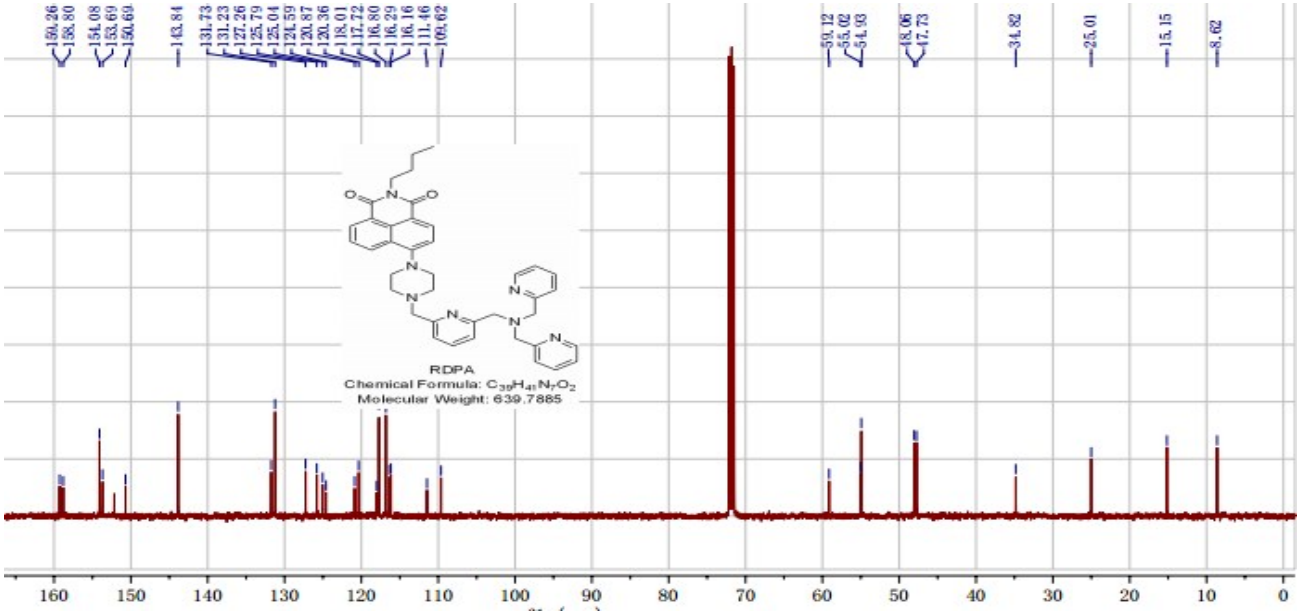

Fig S17. ^{13}C NMR spectrum of **RDPA** in $CDCl_3$.

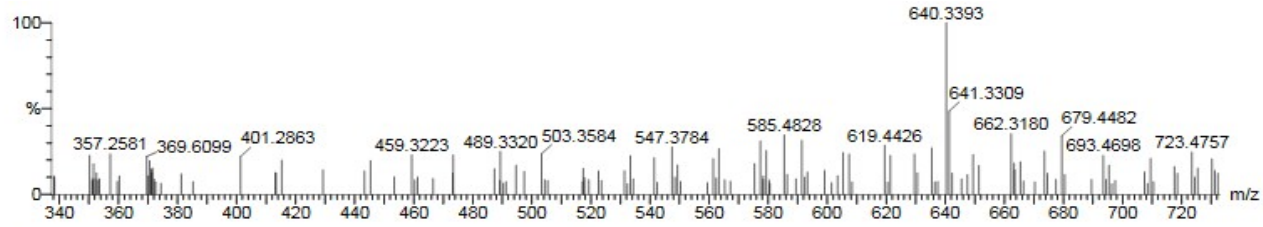

Minimum:		300.0	50.0	-1.5			
Maximum:				100.0			
Mass	Calc. Mass	mDa	PPM	DBE	i-FIT	i-FIT (Norm)	Formula
640.3393	640.3400	-0.7	-1.1	22.5	9.9	0.0	C39 H42 N7 O2

Fig S18. ESI-MS spectrum of **RDPA**

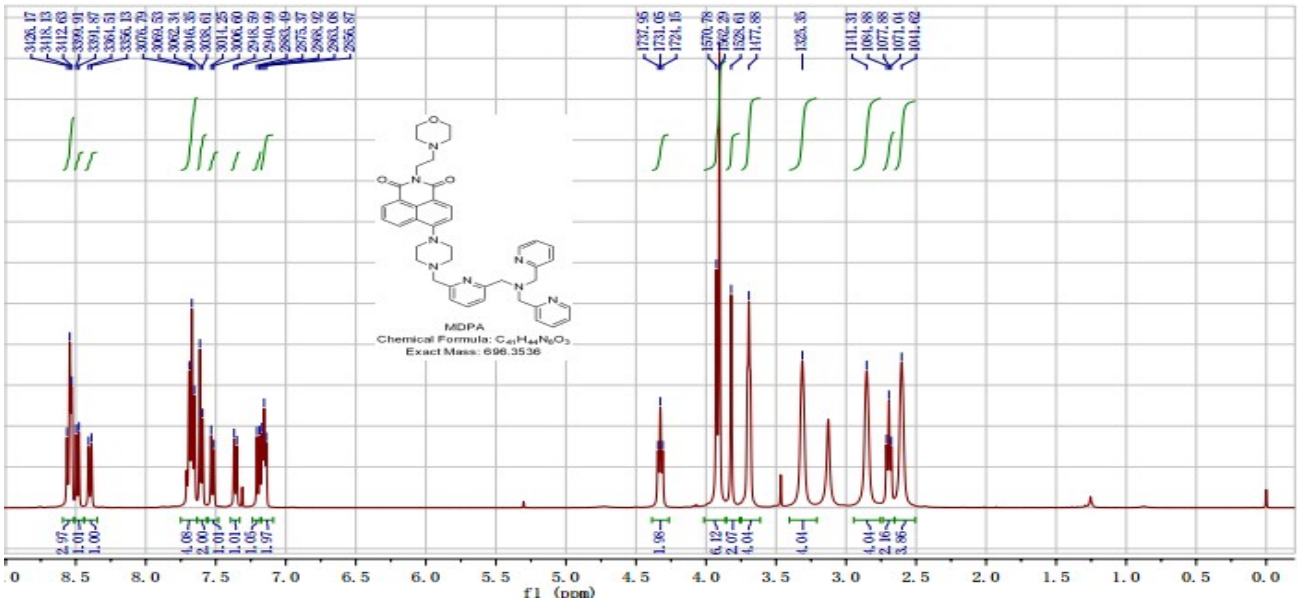

Fig S19. ^{1}H NMR spectrum of **MDPA** in $CDCl_3$.

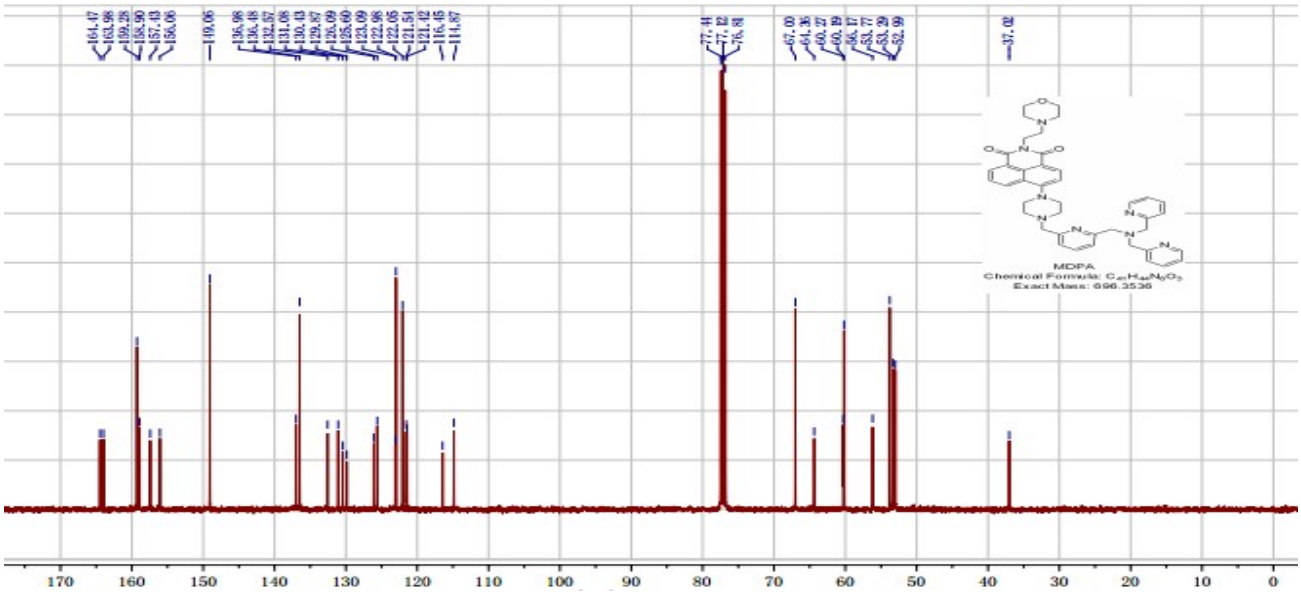

Fig S20. ^{13}C NMR spectrum of **MDPA** in $CDCl_3$.

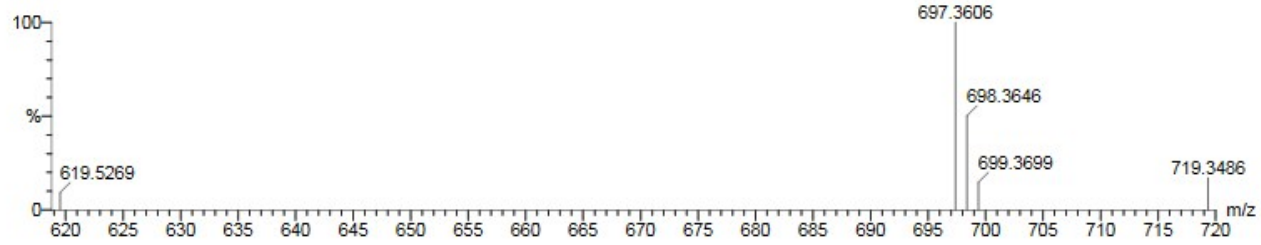

Minimum:				-1.5			
Maximum:		300.0	50.0	100.0			
Mass	Calc. Mass	mDa	PPM	DBE	i-FIT	i-FIT (Norm)	Formula
697.3606	697.3615	-0.9	-1.3	23.5	7.8	0.0	C41 H45 N8 O3

Fig S21. ESI-MS spectrum of **MDPA**

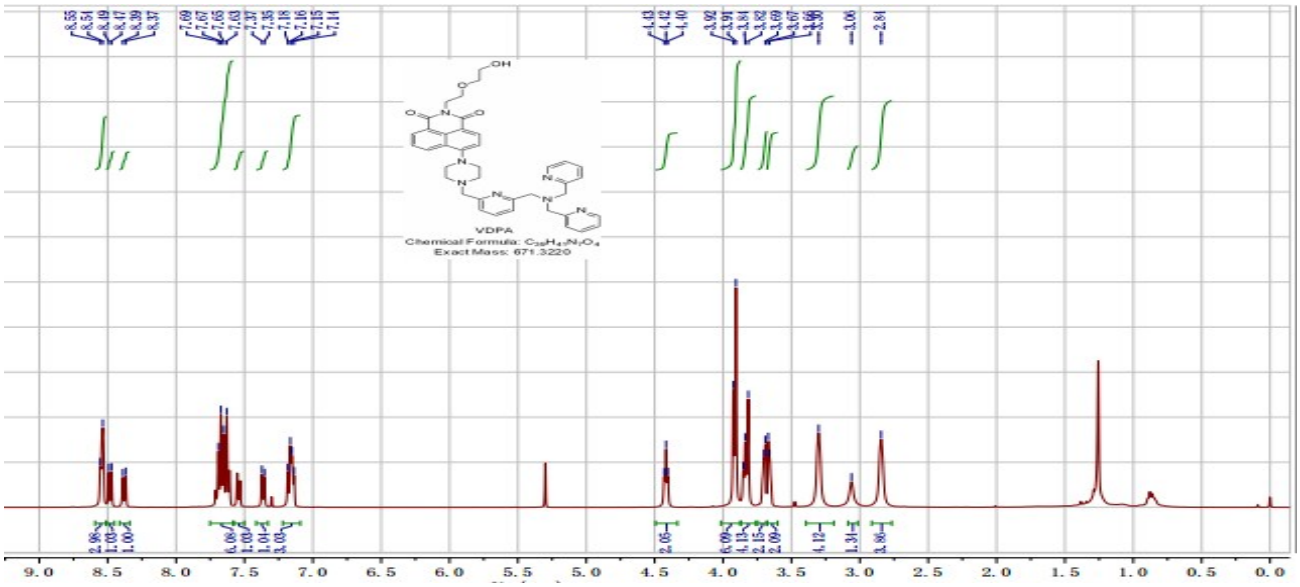

Fig S22. ^{1}H NMR spectrum of **VDPA** in $CDCl_3$.

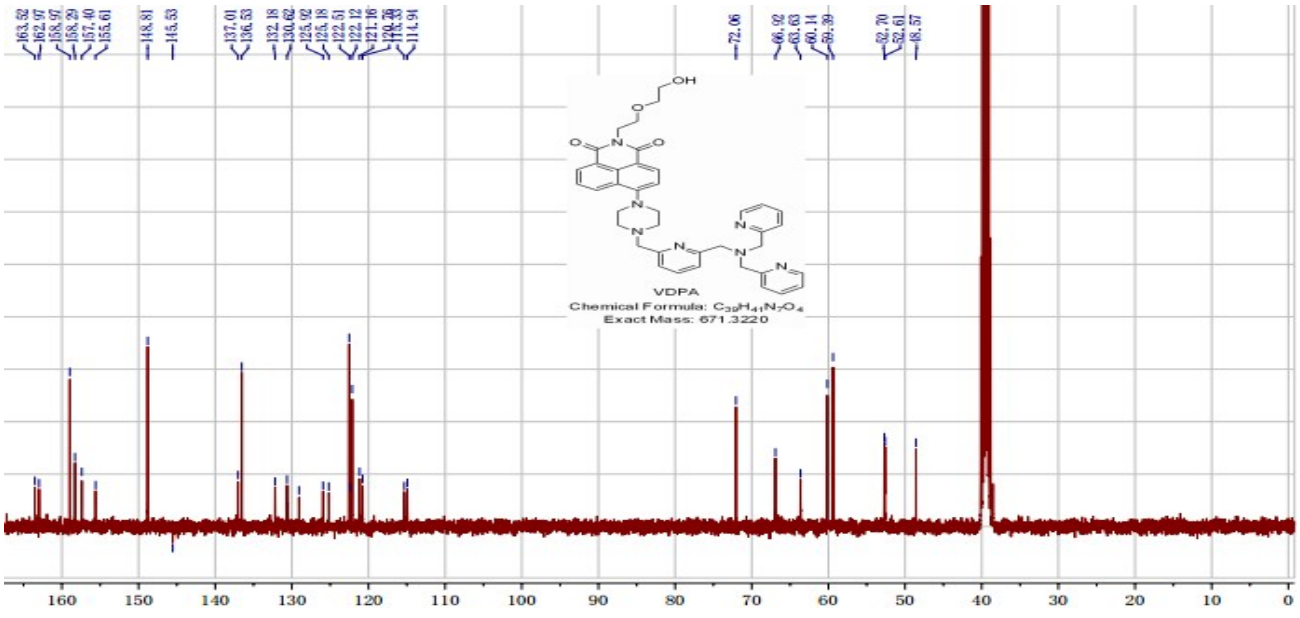

Fig S23. ^{13}C NMR spectrum of **VDPA** in $CDCl_3$.

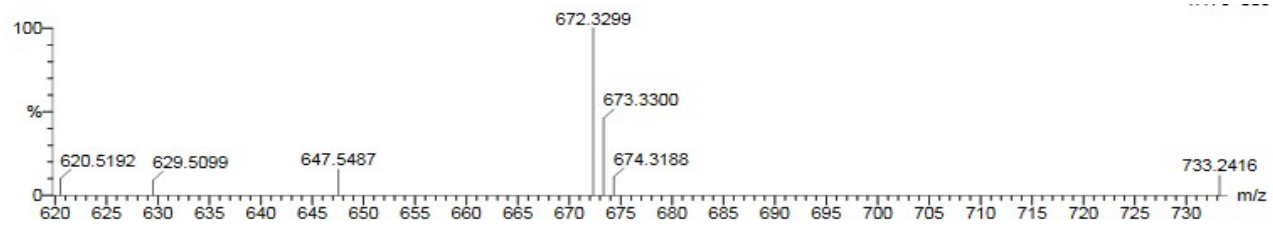

Minimum:				-1.5			
Maximum:		300.0	50.0	100.0			
Mass	Calc. Mass	mDa	PPM	DBE	i-FIT	i-FIT (Norm)	Formula
672.3299	672.3298	0.1	0.1	22.5	8.4	0.0	C39 H42 N7 O4

Fig S24. ESI-MS spectrum of **VDPA**.

6. References

1 (a)V. S. I. Sprakel, J. A. A. W. Elemans, M. C. Feiters, B. Lucchese, K. D. Karlin and R. J. M. Nolte, *Eur. J. Org. Chem.*, 2006, **2006**, 2281-2295; (b)B. Lucchese, K. J. Humphreys, D.-H. Lee, C. D. Incarvito, R. D. Sommer, A. L. Rheingold and K. D. Karlin, *Inorg. Chem.*, 2004, **43**, 5987-5998.

2 G. K. Walkup, S. C. Burdette, S. J. Lippard and R. Y. Tsien, *J. Am, Chem. Soc.*, 2000, **122**, 5644-5645.

3 (a)L. Xu, Y. Xu, W. Zhu, C. Yang, L. Han and X. Qian, *Dalton Trans*, 2012, **41**, 7212-7217; (b)X. Guo, X. Qian and L. Jia, *J. Am. Chem.Soc.*, 2004, **126**, 2272-2273.

4 X. Peng, J. Du, J. Fan, J. Wang, Y. Wu, J. Zhao, S. Sun and T. Xu, *J.Am. Chem. Soc.*, 2007, **129**, 1500-1501.

5 T. Mosmann, *J.Immunol. Methods.*, 1983, **65**, 55-63.